HHS Public Access

Author manuscript

Nanoscale. Author manuscript; available in PMC 2016 November 21.

Published in final edited form as:

Nanoscale. 2015 November 21; 7(43): 18010–18014. doi:10.1039/c5nr04867b.

Anti-HER2/neu Peptide-Conjugated Iron Oxide Nanoparticles for Targeted Delivery of Paclitaxel to Breast Cancer Cells

Qingxin Mu[a], **Forrest M. Kievit**[b], **Rajeev J. Kant**[a], **Guanyou Lin**[c], **Mike Jeon**[a], and **Miqin Zhang**[*,a]

[a] Department of Materials Science and Engineering, University of Washington, Seattle, Washington, 98195, USA

[b] Department of Neurological Surgery, University of Washington, Seattle, Washington, 98195, USA

[c] Department of Bioengineering, University of Washington, Seattle, Washington, 98195, USA

Abstract

Nanoparticles (NPs) for targeted therapy are required to have appropriate size, stability, drug loading and release profiles, and efficient targeting ligands. However, many of existing NPs such as albumin, liposomes, polymers, gold NPs, etc. encounter size limit, toxicity and stability issues when loaded with drugs, fluorophores, and targeting ligands. Furthermore, antibodies are bulky and can greatly affect the physicochemical properties of the NPs, whereas many small molecule-based targeting ligands lack specificity. Here, we report utilization of biocompatible, biodegradable, small (~30 nm) and stable iron oxide NPs (IONPs) for targeted delivery of paclitaxel (PTX) to HER2/neu positive breast cancer using an anti-HER2/neu peptide (AHNP) targeting ligand. We demonstrate the uniform size and high stability of these NPs in biological medium, effective tumour targeting in live mice, as well as their efficient cellular targeting and selective killing in human HER2/neu-positive breast cancer cells.

Breast cancer is the most common cancer in women. Despite significant advances in breast cancer therapy over the past two decades, breast cancer still results in approximately 40,730 deaths per year in the US alone.[1] Along with surgery, breast cancer is commonly treated with radiation, chemo, hormone, and/or targeted therapies.[2-4] However, survival from metastatic breast cancer remains low (23.3%) and thus innovative treatment strategies are urgently needed.[5] Nanotechnology-based strategies for targeted therapies have recently shown promise in breast cancer therapy, including albumin, polymeric, silica, and gold, carbon, and lipid-based nanoparticles (NPs), and some are currently in clinical use.[6-11] For example, paclitaxel (PTX) loaded albumin-stabilized NPs (Abraxane) is an FDA-approved formulation for breast cancer treatment. Abraxane improves the treatment effectiveness and reduces side effects of PTX. However, these NPs have a size of ~130 nm,[6] larger than the size range (10-100 nm) for optimal in vivo navigation of nanomedicines and have no active targeting mechanism to promote target cell internalization.[12-14] Furthermore, NPs made of

[*] *mzhang@uw.edu*.

† Electronic Supplementary Information (ESI) available. See DOI: 10.1039/x0xx00000x

gold, polymeric, silica and carbon materials and liposomes often suffer issues of toxicity, biodegradability, size limit, and stability when loaded with the drugs, fluorophores, and/or targeting ligands required for effective therapy.[15, 16]

Anti-human epidermal growth factor receptor 2 (HER2/neu) monoclonal antibodies are commonly used for breast cancer targeting as ~25% of breast cancer patients display overexpression of HER2/neu, and have been used for targeted therapy.[17, 18] Many HER2-targeting NP-based drug/gene delivery systems utilize anti-HER2/neu antibodies such as trastuzumab as targeting ligands.[19-21] Monoclonal antibodies have distinct advantages as targeting ligands over small molecules, proteins, and aptamers due to their homogeneity, affinity, and specificity. However, their large size can dramatically alter the physicochemical properties of NPs and affect pharmacokinetics when they are attached to NPs. The anti-HER2/neu peptide (AHNP) is a small exocyclic peptide derived from the anti-p185HER2/neu monoclonal antibody, trastuzumab. The peptide binds to the HER2/neu receptor with high affinity (300 nM) and also inhibits the kinase activity.[22] Attachment of AHNP to NPs or drugs has been shown to provide effective targeting and internalization into HER2/neu+ cells.[23, 24] However, none of existing AHNP-based NP drug delivery systems have demonstrated effective *in vivo* tumour targeting and selective HER2 positive cancer cell killing. Herein, we report an AHNP-conjugated and PTX-loaded iron oxide NP (IONP-PTX-AHNP) for targeted treatment of HER2/neu positive breast cancer that maintains high stability and biocompatibility. We also conjugated carboxymethylated-β-cyclodextrin (CM-β-CD) onto IONPs to allow hydrophobic loading of PTX (Figure 1). IONP can aid in tumour imaging and treatment monitoring through magnetic resonance imaging (MRI).[25, 26] We characterized NPs with transmission electron microscopy (TEM), dynamic light scattering (DLS), and high performance liquid chromatography-mass spectroscopy (HPLC-MS). We also evaluated their stability and drug release behaviour as well as in vivo tumour targeting efficiency. selective cellular uptake and cancer cell killing activities of IONP-PTX-AHNP.

Polyethylene glycol (PEG) monolayer-coated IONPs (IONP-PEG-NH2) were prepared according to our previously reported approach,[27] followed by the chemical attachment of AHNP and CM-β-CD following a similar procedure reported previously.[28] PTX was loaded into the NPs through hydrophobic interaction with CD to obtain IONP-PTX-AHNP. The resulting IONP-PTX-AHNP was imaged with transmission electron microscopy (TEM) with and without negative staining with uranyl acetate (Fig. 2). TEM images showed that IONP-PTX-AHNP had a uniform core size of ~12 nm. Without negative staining, some surface coating could be observed surrounding the iron cores (Fig. 2a, left, inset). With negative staining, the surface coating was not stained and could be visualized as a ~2.5 nm white border surrounding the iron core. DLS showed IONP-PTX-AHNP had a hydrodynamic diameter of 30.2 nm in PBS with high monodispersity (PDI = 0.08). To be an effective cancer treatment, NPs must maintain stability in biologically relevant buffers. IONP-PTX-AHNP was added into cell culture medium containing serum proteins and maintained for two weeks while the hydrodynamic size was monitored. Results show that these NPs had great stability in the biological medium as evidenced by their minimal change in hydrodynamic size (Fig. 2b and c), similar to our previous study using IONPs for brain cancer treatment.[28] The zeta potential of IONP-PTX-AHNP was slightly negative, which is

ideal for a targeting NP.[29, 30] Loading of PTX was quantified by high-performance liquid chromatography (HPLC) after acetonitrile extraction from NPs (Fig. 2d), which revealed that there were ~274 PTX molecules per NP (based on ~0.64 nmol NP per mg Fe). The percentage of PTX loading was ~14.7% (mg PTX/mg Fe), which falls in the range of many other NP systems.[31-33] Additionally, there were ~170 AHNP molecules per NP as quantified by HPLC-MS (Fig. S1).

Drug release was accessed using dialysis and quantified by HPLC. At pH 7.4, IONP-PTX-AHNP showed a slow release profile with only 66.7% of PTX released after 48 h incubation. However, at pH 5.4, an increased drug release was observed with a ~90% of PTX released after 48 h incubation, and a burst release of ~13% PTX after 1 h incubation. This result indicates that the release of PTX in blood would be slow, but greatly accelerate once entering acidic cellular compartments such as endosomes. Since PTX does not have any ionisable groups with pKa values in the physiological range, the lower pH would not be expected to change the ionic state of the drug and thus its dissociate constant from CM-β-CD.[34] Rather, the pH change likely affected hydrogen bonding between PTX and CM-β-CD and the physical stability of PTX on NP.[35] According to their chemical structures, PTX has 4 hydrogen bond donors and 14 acceptors, and the native β-CD has 21 donors and 35 acceptors. Many of these hydrogen bonds may contribute to the pH-responsive drug release. Drug release during the first hour was faster than the following hours, which was likely due to a higher initial drug gradient between NPs and solution. As drug gradually was released, the gradient declined and the rate decreased. In vivo targeting of AHNP-conjugated IONPs was tested in a human HER2/neu+ SK-BR-3 breast cancer xenograft mouse model.[36] A near-infrared dye, Cy5.5-NHS, was conjugated onto free amine of IONPs after AHNP conjugation (IONP-AHNP-Cy5.5) for imaging purposes. Cells were inoculated into flanks of athymic nude mice and NPs were injected nine days after the inoculation when tumours were observed and approximately 42 mm^3 in size. The AHNP-targeting NPs accumulated in tumours within 6 hrs after the injection and were retained for at least 72 hrs (red dashed circles in Fig. 3a). Fluorescence signal was also detected in other organs such as brain, liver, spleen and spine. These signals started to decline at 96 h suggesting elimination. We also applied a non-targeting NP control to separate active targeting from passive targeting caused by the enhanced permeability and retention (EPR) effect. With the control NPs, minimal signal was observed in tumour. The signal from tumours and whole bodies were quantified and the radiant efficiency ratios of tumour to whole body were compared between targeting and control groups. The targeting group showed drastically higher ratios than the controls group, showing a 2.5-fold increase in signal for the targeting NPs as compared to the non-targeting NPs. This shows AHNP provides excellent targeting *in vivo* when attached to IONPs. AHNP was covalently conjugated onto IONPs, and not designed to release in the blood or tumours according to the conjugation chemistry. Therefore, fate of free AHNP would not affect the in vivo behaviour of IONP-AHNP-Cy5.5. Indeed, AHNP has a very short blood half-life (< 30 min).[37] Therefore, the free peptide would be mostly cleared from blood at the first measurement time point (i.e., 6 h after NP injection).

To evaluate the therapeutic efficacy of the NPs, in vitro studies were conducted using two human breast cancer cell lines: SK-BR-3 and MDA-MB-231. These two cell types are reported to have high (SK-BR-3) and low (MDA-MB-231) HER2/neu expressions and have

been widely used in HER2 targeting studies.[36, 38] To visualize cell uptake, IONP-PTX-AHNP was labelled with Cy5. IONP-PTX-AHNP-Cy5 was incubated with cells for 1 hr at 40 μg Fe/mL in cell culture medium. Uptake of NPs into cells was imaged with confocal laser scanning microscopy (CLSM) using a Leica SP8 microscope. Significant targeting was achieved in SK-BR-3 cells where fluorescence was observed within cells incubated with NPs. MDA-MB-231 cells showed no fluorescence from the NPs indicating uptake was specific to HER2/neu+ cells. To quantify the difference in cell uptake, we used flow cytometry to analyse the fluorescence intensity of treated cells. The mean fluorescence intensity in SK-BR-3 cells showed a 4-fold increase over MDA-MB-231. This result is consistent with CLSM images and indicates uptake of AHNP targeted NPs is specific to HER2/neu expressing cells.

An Alamar Blue cell viability assay was used to test the cell killing of free PTX, IONP-PTX-AHNP and IONP-AHNP (NP control without PTX) with the two breast cancer cell lines. Cells were treated with free PTX or IONP-PTX-AHNP at the same concentrations of PTX for 3 days. For cells treated with IONP-AHNP, identical iron concentrations as IONP-PTX-AHNP were used. Result showed that IONP-AHNP alone didn't affect cell viability at all concentrations indicating its biocompatibility. Both PTX and IONP-PTX-AHNP showed effective cell killing in both cell lines. However, IONP-PTX-AHNP showed enhanced cell killing only in SK-BR-3 cells whereas free PTX showed similar cell killing in both cell lines. At a PTX concentration of 2.5 nM, IONP-PTX-AHNP induced nearly 30% enhancement of killing in SK-BR-3 cells compare to MDA-MB-231 cells. Although the IC50s of PTX in two cell lines were both ~10 nM, the IC50 of IONP-PTX-NP in MDA-MB-231 cells was ~14 nM, ~20-fold higher than that in SK-BR-3 cells (~0.7 nM). This indicates that the enhanced cell uptake mediated by the targeting ligand AHNP to PTX-loaded IONP was able to improve treatment of HER2/neu+ breast cancer cells. As breast cancer patients have a widely-varied HER2 expression levels,[36] further in depth study using cell lines with different HER2 expression levels will be required to fully elucidate minimum HER2 expression for effective targeted therapy.

Conclusions

In summary, we have explored an IONP-based, anti-HER2/neu peptide conjugated and PTX-loaded NP that possesses small size and uniform shape, and great stability in biological medium. Significantly, this NP formulation showed great in vivo and in vitro targeting capability towards human HER2/neu-positive breast cancer cells and significant enhancement in cell killing.

Supplementary Material

Refer to Web version on PubMed Central for supplementary material.

Acknowledgements

The work is supported by NIH grants R01CA161953 and R01CA134213. Q. M. acknowledges support from an NIH Ruth L. Kirschstein T32 Fellowship (T32CA138312). We acknowledge technical assistance from Victoria K. Patton in the Department of Chemical Engineering and Christopher J. Dayringer in the Department of Materials Science and Engineering.

Notes and references

1. Siegel RL, Miller KD, Jemal A. CA: A Cancer Journal for Clinicians. 2015; 65:5–29. [PubMed: 25559415]
2. Veiseh O, Sun C, Fang C, Bhattarai N, Gunn J, Kievit F, Du K, Pullar B, Lee D, Ellenbogen RG, Olson J, Zhang M. Cancer Research. 2009; 69:6200–6207. [PubMed: 19638572]
3. Veiseh O, Sun C, Gunn J, Kohler N, Gabikian P, Lee D, Bhattarai N, Ellenbogen R, Sze R, Hallahan A, Olson J, Zhang M. Nano Letters. 2005; 5:1003–1008. [PubMed: 15943433]
4. Piccart-Gebhart MJ, Procter M, Leyland-Jones B, Goldhirsch A, Untch M, Smith I, Gianni L, Baselga J, Bell R, Jackisch C, Cameron D, Dowsett M, Barrios CH, Steger G, Huang C-S, Andersson M, Inbar M, Lichinitser M, Láng I, Nitz U, Iwata H, Thomssen C, Lohrisch C, Suter TM, Rüschoff J, Sütő T, Greatorex V, Ward C, Straehle C, McFadden E, Dolci MS, Gelber RD. New Engl. J. Med. 2005; 353:1659–1672. [PubMed: 16236737]
5. Siegel R, DeSantis C, Virgo K, Stein K, Mariotto A, Smith T, Cooper D, Gansler T, Lerro C, Fedewa S, Lin C, Leach C, Cannady RS, Cho H, Scoppa S, Hachey M, Kirch R, Jemal A, Ward E. CA: A Cancer Journal for Clinicians. 2012; 62:220–241. [PubMed: 22700443]
6. Miele E, Spinelli GP, Miele E, Tomao F, Tomao S. International Journal of Nanomedicine. 2009; 4:99–105. [PubMed: 19516888]
7. Pridgen EM, Langer R, Farokhzad OC. Nanomedicine. 2007; 2:669–680. [PubMed: 17976029]
8. Tsai C-P, Chen C-Y, Hung Y, Chang F-H, Mou C-Y. J. Mater. Chem. 2009; 19:5737–5743.
9. Kodiha M, Hutter E, Boridy S, Juhas M, Maysinger D, Stochaj U. Cell. Mol. Life Sci. 2014; 71:4259–4273. [PubMed: 24740795]
10. Shao W, Paul A, Zhao B, Lee C, Rodes L, Prakash S. Biomaterials. 2013; 34:10109–10119. [PubMed: 24060420]
11. Weiner N, Martin F, Riaz M. Drug Dev. Ind. Pharm. 1989; 15:1523–1554.
12. Zhao L, Seth A, Wibowo N, Zhao C-X, Mitter N, Yu C, Middelberg APJ. Vaccine. 2014; 32:327–337. [PubMed: 24295808]
13. Chauhan VP, Stylianopoulos T, Martin JD, Popovic Z, Chen O, Kamoun WS, Bawendi MG, Fukumura D, Jain RK. Nat Nano. 2012; 7:383–388.
14. Nie S. Nanomedicine (London, England). 2010; 5:523–528.
15. Mu Q, Jiang G, Chen L, Zhou H, Fourches D, Tropsha A, Yan B. Chemical Reviews. 2014; 114:7740–7781. [PubMed: 24927254]
16. Sharma A, Sharma US. International Journal of Pharmaceutics. 1997; 154:123–140.
17. Ito A, Kuga Y, Honda H, Kikkawa H, Horiuchi A, Watanabe Y, Kobayashi T. Cancer Lett. 2004; 212:167–175. [PubMed: 15279897]
18. Lewis Phillips GD, Li G, Dugger DL, Crocker LM, Parsons KL, Mai E, Blättler WA, Lambert JM, Chari RVJ, Lutz RJ, Wong WLT, Jacobson FS, Koeppen H, Schwall RH, Kenkare-Mitra SR, Spencer SD, Sliwkowski MX. Cancer Res. 2008; 68:9280–9290. [PubMed: 19010901]
19. Colombo M, Corsi F, Foschi D, Mazzantini E, Mazzucchelli S, Morasso C, Occhipinti E, Polito L, Prosperi D, Ronchi S, Verderio P. Pharmacol. Res. 2010; 62:150–165. [PubMed: 20117211]
20. Ngamcherdtrakul W, Morry J, Gu S, Castro DJ, Goodyear SM, Sangvanich T, Reda MM, Lee R, Mihelic SA, Beckman BL, Hu Z, Gray JW, Yantasee W. Adv. Funct. Mater. 2015; 25:2646–2659. [PubMed: 26097445]
21. Zhou Z, Badkas A, Stevenson M, Lee J-Y, Leung Y-K. Int. J. Pharm. 2015; 487:81–90. [PubMed: 25865568]
22. Park B-W, Zhang H-T, Wu C, Berezov A, Zhang X, Dua R, Wang Q, Kao G, O'Rourke DM, Greene MI, Murali R. Nat Biotech. 2000; 18:194–198.
23. Zhanzhang Wang ZY, Xianrong Qi. Journal of Chinese Pharmaceutical Sciences. 2013; 22:441–448.
24. Guillemard V, Nedev HN, Berezov A, Murali R, Saragovi HU. DNA Cell Biol. 2005; 24:351–358.
25. Kievit FM, Veiseh O, Fang C, Bhattarai N, Lee D, Ellenbogen RG, Zhang M. ACS Nano. 2010; 4:4587–4594. [PubMed: 20731441]

26. Fang C, Veiseh O, Kievit F, Bhattarai N, Wang F, Stephen Z, Li C, Lee D, Ellenbogen RG, Zhang M. Nanomedicine. 2010; 5:1357–1369. [PubMed: 21128719]
27. Fang C, Bhattarai N, Sun C, Zhang MQ. Small. 2009; 5:1637–1641. [PubMed: 19334014]
28. Mu Q, Jeon M, Hsiao M-H, Patton VK, Wang K, Press OW, Zhang M. Advanced Healthcare Materials. 2015; 4:1236–1245. [PubMed: 25761648]
29. Xiao K, Li Y, Luo J, Lee JS, Xiao W, Gonik AM, Agarwal RG, Lam KS. Biomaterials. 2011; 32:3435–3446. [PubMed: 21295849]
30. Kim B, Han G, Toley BJ, Kim C.-k. Rotello VM, Forbes NS. Nat Nano. 2010; 5:465–472.
31. Zhang Z, Mei L, Feng S-S. Expert Opinion on Drug Delivery. 2013; 10:325–340. [PubMed: 23289542]
32. Zhao D, Zhao X, Zu Y, Li J, Zhang Y, Jiang R, Zhang Z. International Journal of Nanomedicine. 2010; 5:669–677. [PubMed: 20957218]
33. Jia L, Shen J, Li Z, Zhang D, Zhang Q, Duan C, Liu G, Zheng D, Liu Y, Tian X. Int. J. Pharm. 2012; 439:81–91. [PubMed: 23078857]
34. Stella VJ, Rao VM, Zannou EA, Zia V. Advanced Drug Delivery Reviews. 1999; 36:3–16. [PubMed: 10837705]
35. Amini-Fazl MS, Mobedi H, Barzin J. Drug Development and Industrial Pharmacy. 2014; 40:519–526. [PubMed: 23594296]
36. Subik K, Lee J-F, Baxter L, Strzepek T, Costello D, Crowley P, Xing L, Hung M-C, Bonfiglio T, Hicks DG, Tang P. Breast Cancer : Basic and Clinical Research. 2010; 4:35–41. [PubMed: 20697531]
37. Su Z. Journal of Labelled Compounds & Radiopharmaceuticals. 2006; 49:1259–1271.
38. Fantin VR, Berardi MJ, Babbe H, Michelman MV, Manning CM, Leder P. Cancer Research. 2005; 65:6891–6900. [PubMed: 16061673]

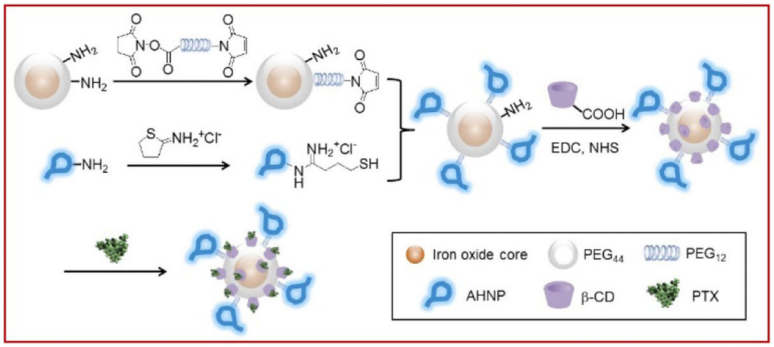

Significantly, we examined the

Fig. 1.
Schematic illustration of IONP-PTX-AHNP synthesis.

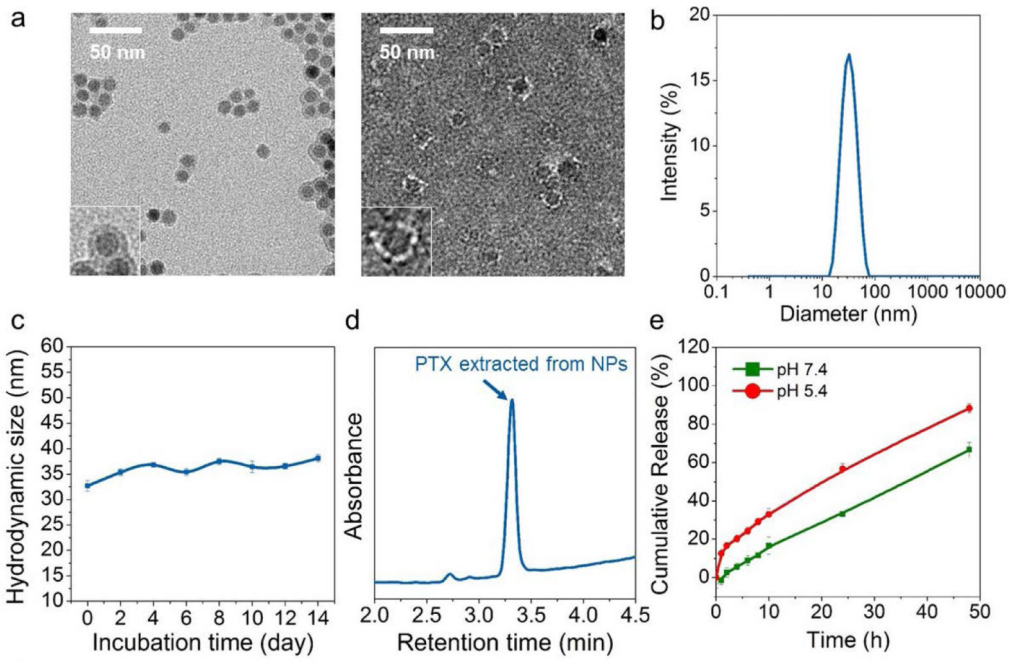

f

	Core size (nm)	Z-average size (nm)	PDI	ζ-potential (pH 7.4) (mV)	PTX per NP	AHNP per NP
IONP-PTX-AHNP	14.4 ± 1.5	30.8	0.08	-4.59	~274	~170

Fig. 2.

Characterization of IONP-PTX-AHNP. a. TEM micrographs of NPs without (left) and with (right) negative staining. Insets: enlarged images; Scale bars: 50 nm; b. DLS analysis of NPs in PBS; c. Stability of NPs in complete cell culture medium (DMEM + 10% FBS + antibiotics); d. HPLC analysis of PTX extracted from NPs; e. cumulative drug release of PTX from NPs at pH 7.4 (green line, PBS + 0.1% Tween 80) and pH 5.4 (red line, sodium acetate buffer + 0.1% Tween 80); f. Properties of IONP-PTX-AHNP.

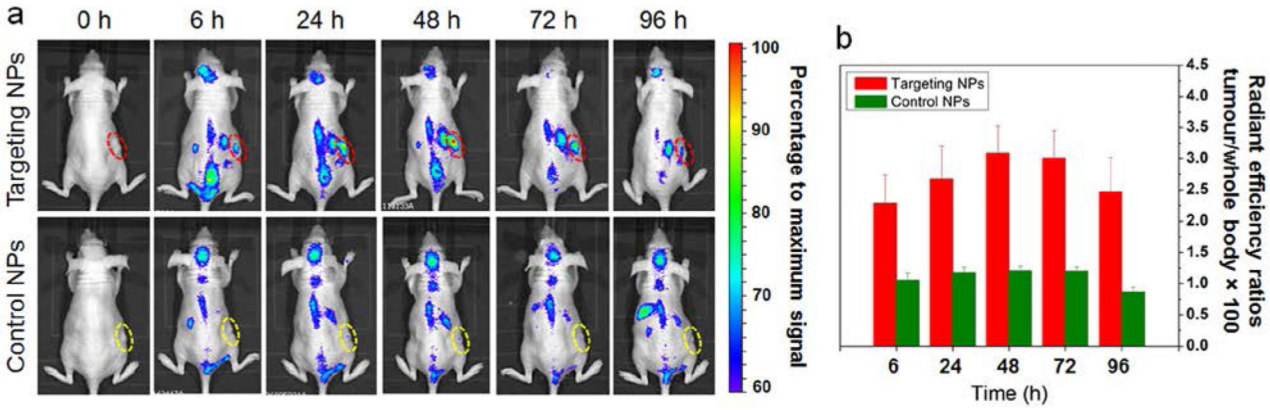

Fig. 3.

Effective in vivo targeting of HER2/neu+ SK-BR-3 breast cancer in living mice by AHNP-conjugated IONPs. IONP-AHNP-Cy5.5 or IONP-Cy5.5 was injected into mice intravenously (NPs amount equivalent to 0.5 mg Fe). Fluorescence images were taken immediately before NP injection and 6, 24, 48, 72 and 96 h after injections. a. Fluorescence images of mice after NP injections. Fluorescence intensity at different time points and two groups was normalized to same scale. Red and yellow dashed circles indicate tumours; b. Percentages of radiant efficiency in tumour to whole body at different time points. Error bars represent standard deviation and are from three independent measurements.

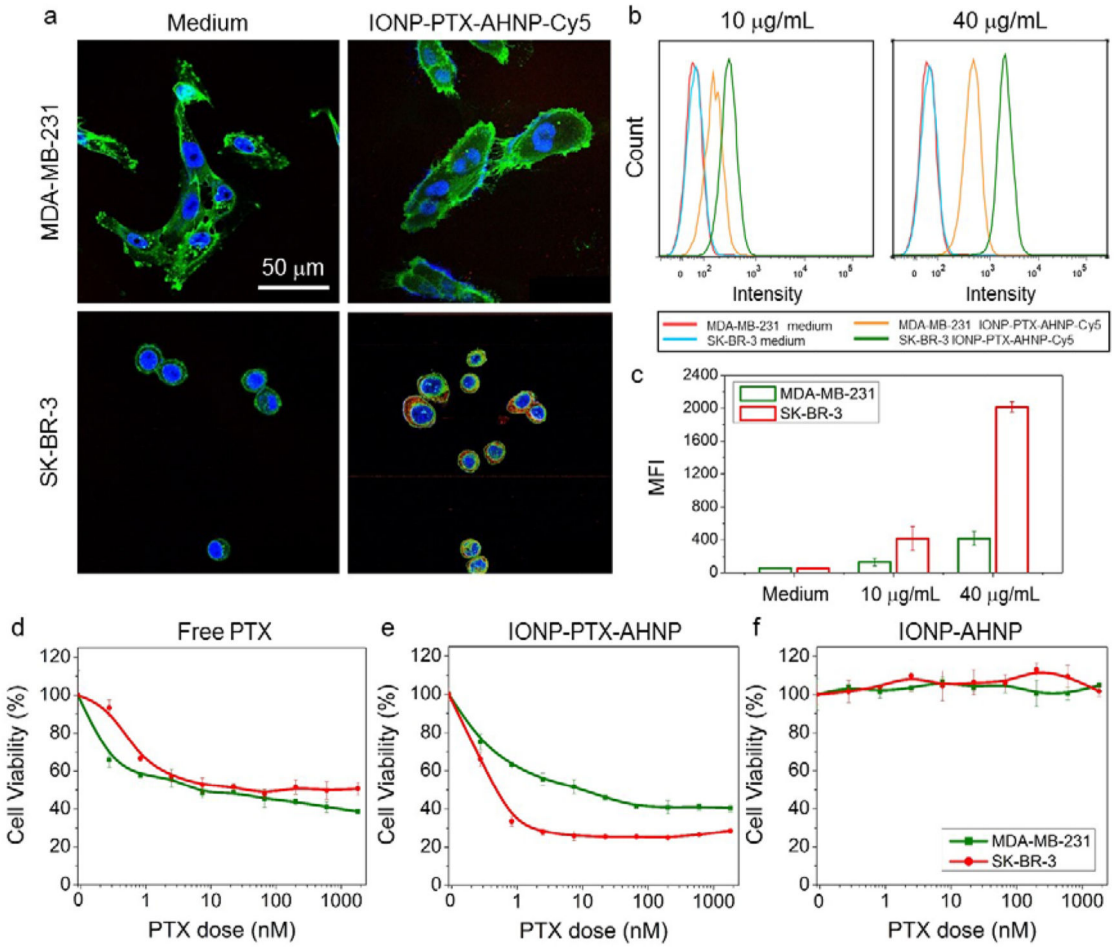

Fig. 4.

In vitro evaluation of NPs. A. CLSM images of cells incubated with medium or IONP-PTX-AHNP-Cy5. Blue: cell nucleus (DAPI); Green: cell membrane (WGA-Alexa Fluor 555, false-coloured); Red: IONP-PTX-AHNP-Cy5 (false-coloured); b. analysis of cell uptake of NPs in two cell lines by flow cytometry; c. MFI of two cell types incubated with NPs; d-f, viability of MDA-MB-231 (green curves) and SK-BR-3 (red curves) after 72 hrs treatment of free PTX (d), IONP-PTX-AHNP (e) or IONP-AHNP (f). PTX doses were 1800, 600, 200, 66.7, 22.2, 7.4, 2.5, 0.82 and 0.27 nM for PTX and IONP-PTX-AHNP. Iron concentrations of IONP-AHNP were equivalent to those in IONP-PTX-AHNP treatments.